

ANALYSIS OF LGS RESONATORS USING THE FINITE PLATE TECHNIQUE

Irina Mateescu¹, John Kosinski², Robert Pastore², Gary Johnson³

Liviu Dumitrache¹, Lucian Gheorghe⁴, Cristina Bran¹

¹National Institute of Materials Physics, Bucharest-Magurele, Romania

²US Army CECOM, Fort Monmouth, NJ, USA

³Sawyer Research Products, Eastlake, Ohio, USA

⁴National Institute for Lasers, Plasma and Radiations Physics, Bucharest-Magurele, Romania

Abstract – This paper presents the results of an analysis using the finite plate technique of Y-cut langasite plan-parallel resonators with Al and Ag electrodes. We have extracted values for the piezoelectrically stiffened elastic stiffness c_{66}^D , the elastic stiffness c_{66}^E , the piezoelectric stress constant e_{11} , and the dielectric permittivity ϵ_{11}^S . The measured material constants are in very good agreement with other reported values. This paper will present our new results on the langasite samples, and will include a comparison between an analysis of the data using the measurement method recommended by the current IEEE Standard on Piezoelectricity and the finite plate technique.

Key words - langasite, material constants, energy trapping

I. INTRODUCTION

Some of the basic resonator method measurands of the IEEE Standard on Piezoelectricity [1] are strongly affected by the non-uniform distribution of vibratory motion found in practical plate resonators. As a consequence, piezoelectric material constants determined using this method may be significantly in error. Based on Ballato's exact transmission-line analogs [2], an improved resonator method for the determination of piezoelectric material constants ("finite plate technique") was developed [3]. In this technique, the constants of interest are extracted from a self-consistent analysis of multiple harmonics using Ballato's exact transmission-line analogs.

This paper presents the results of an analysis using the finite plate technique of Y-cut langasite plan-parallel resonators with Al and Ag electrodes. We have extracted values for the piezoelectrically stiffened elastic stiffness c_{66}^D , elastic stiffness c_{66}^E , piezoelectric stress constant e_{11} , and dielectric permittivity ϵ_{11}^S . The measured material constants are in very good agreement with other reported values. This paper presents our new results on the langasite samples, and includes a comparison between an analysis of the data using the measurement method recommended by the current IEEE Standard on Piezoelectricity and the finite plate technique.

II. EXPERIMENTAL SAMPLES

Our experimental samples were nine nominally Y-cut Sawyer langasite plates. The samples were plan-parallel polished plates of nominally 14 mm diameter and approximately 4 or 5 MHz fundamental resonant frequency. The as-cut langasite wafers were lapped with 3 μ m alumina powder. Between lapping and polishing steps, the langasite wafers were chemically etched in a 2HNO₃:CH₃COOH solution for removal of any disturbed layer due to the mechanical treatment. The polishing process used a slurry of colloidal alkaline suspension of silica gel (QUSO) on a Politec pad material [4].

Electrodes were deposited by thermal evaporation in vacuum using a JEOL - JEE 4X installation. All electrodes were 7 mm in diameter. One set of four plates received 330 nm thick Al electrodes and the other set of five plates received 150 nm thick Ag electrodes. These electrode thicknesses correspond to relatively low nominal mass loading values of 0.11% and 0.17% respectively. The dimensions, masses, and densities of the individual plates were determined as listed in Tables I and II. Also listed in Tables I and II are the static (parallel plate) capacitance values of the electroded plates

TABLE I
SUBSTRATE DATA FOR THE Al-ELECTRODED RESONATORS

Sample	Diameter (mm)	2h (mm)	Mass (g)	Density (g/cm ³)	C ₀ (pF)
1	14.08	0.276	0.2408	5604	26.07
2	14.06	0.274	0.2388	5613	25.21
3	14.08	0.2745	0.2392	5597	25.17
4	14.12	0.275	0.2422	5624	25.71

TABLE II
SUBSTRATE DATA FOR THE Ag-ELECTRODED RESONATORS

Sample	Diameter (mm)	2h (mm)	Mass (g)	Density (g/cm ³)	C ₀ (pF)
1	13.84	0.34	0.2945	5758	21.32
2	13.87	0.339	0.2947	5754	21.09
3	13.85	0.338	0.293	5754	20.87
4	13.83	0.341	0.2948	5755	21.29
5	13.85	0.34	0.2946	5751	21.06

The resonance and antiresonance frequencies of the fundamental and first three odd harmonic overtones of the slow thickness shear mode were measured using Level Measuring Set PSM-5, Wandel u. Goltermann, Germany. The measured frequencies are listed in Tables III and IV.

III. DATA ANALYSIS

A. Basic Approach

We consider the electroded flat plates to be represented adequately by Ballato's transmission line analogs (see Fig. 1) and associated frequency equations [2]. The series of resonance frequency harmonics $f_{R\mu}^{(M)}$ should fit well to

$$\tan(X) = \frac{X}{k^2 + \mu X^2} \quad (1)$$

while the series of antiresonance harmonics $f_{A\mu}^{(M)}$ should fit well to

$$\tan(X) = \frac{1}{\mu X} \quad (2)$$

where

$$X = \frac{\pi}{2} \frac{f}{f_{A0}^{(1)}} \quad (3)$$

with f as $f_{R\mu}^{(M)}$ and $f_{A\mu}^{(M)}$ respectively in (1) and (2). The quantity $f_{A0}^{(1)}$ represents the fundamental ($M=1$) antiresonance frequency with zero mass loading. The quantity μ denotes the normalized mass loading on each plate surface, calculated from the mass per unit area m as

$$\mu = \frac{m}{\rho h} = \frac{\rho_e t_e}{\rho h} \quad (4)$$

where ρ_e and t_e are respectively the electrode mass density and thickness. The quantity k denotes the piezoelectric coupling.

TABLE III
CRITICAL FREQUENCIES OF THE Al-ELECTRODED RESONATORS

Sample	f	M=1	M=3	M=5	M=7
1	$f_{R\mu}^{(M)}$	5037424	15222986	25391352	35551888
	$f_{A\mu}^{(M)}$	5059830	15225912	25394508	35554766
2	$f_{R\mu}^{(M)}$	5031562	15205574	25361140	35510308
	$f_{A\mu}^{(M)}$	5055344	15208432	25364866	35512928
3	$f_{R\mu}^{(M)}$	5024042	15184976	25326794	35462522
	$f_{A\mu}^{(M)}$	5037078	15188428	25330698	35465784
4	$f_{R\mu}^{(M)}$	5020936	15175598	25311426	35440602
	$f_{A\mu}^{(M)}$	5044942	15178648	25315050	35443720

TABLE IV
CRITICAL FREQUENCIES OF THE Ag-ELECTRODED RESONATORS

Sample	f	M=1	M=3	M=5	M=7
1	$f_{R\mu}^{(M)}$	4041314	12203446	20352754	28494602
	$f_{A\mu}^{(M)}$	4067276	12207188	20357044	28498372
2	$f_{R\mu}^{(M)}$	4043806	12210018	20363744	28510082
	$f_{A\mu}^{(M)}$	4069646	12214178	20368072	28513484
3	$f_{R\mu}^{(M)}$	4041426	12202794	20351276	28491708
	$f_{A\mu}^{(M)}$	4067638	12206442	20355274	28495266
4	$f_{R\mu}^{(M)}$	4043744	12210882	20364566	28510242
	$f_{A\mu}^{(M)}$	4069410	12214472	20368366	28513404

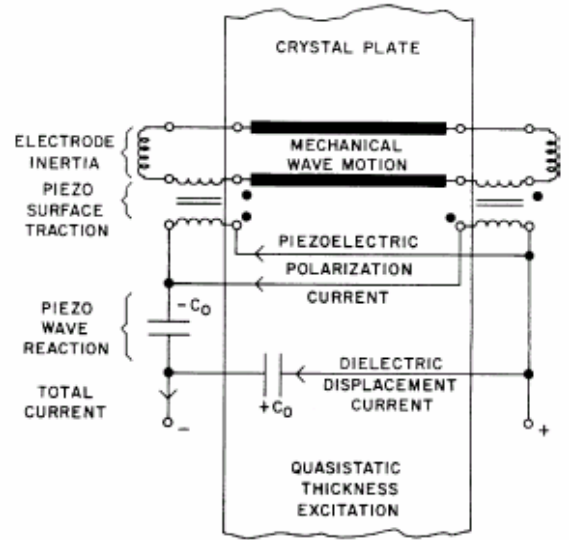


Fig. 1. Exact electrical equivalent network for a single thickness mode driven by thickness-field excitation in a laterally unbounded piezoelectric resonator [2].

For the infinite flat plate, the series of $f_{A\mu}^{(M)}$ depend only upon μ and $f_{A0}^{(1)}$, hence the measurement of $f_{A\mu}^{(M)}$ on four harmonics should over-determine both μ and $f_{A0}^{(1)}$. Similarly, for the infinite flat plate, the series of $f_{R\mu}^{(M)}$ depend only upon k , μ , and $f_{A0}^{(1)}$, hence the measurement of $f_{R\mu}^{(M)}$ on four harmonics should over-determine k , μ and $f_{A0}^{(1)}$. And, of course, the same μ and $f_{A0}^{(1)}$ should be obtained from both the $f_{R\mu}^{(M)}$ and $f_{A\mu}^{(M)}$ series.

In practice, the results obtained for finite plates deviate from those expected for an infinite plate. Most significantly, we expect the coupling to be reduced due to the non-uniform distribution of motion, and we expect the apparent mass loading to differ from the theoretical value [5]. Thus, in part, our analysis here examines the degree to which the simple model accurately represents the measured data, and the corresponding limits within which the model is appropriate for the determination of fundamental as opposed to effective piezoelectric material properties.

B. Interpretation of Frequency Spectra

We begin our analysis with the measured resonance and antiresonance frequencies of the electroded plates. The first step is to estimate the fundamental antiresonance frequency $f_{A0}^{(1)}$ implied by the series of measured $f_{A\mu}^{(M)}$. The simplest approach is to ignore any mass loading and track the convergence of $f_{A\mu}^{(M)}/M$ with increasing harmonic. The next level of sophistication is to examine the differences between successive harmonics, somewhat reducing the errors associated with ignoring the mass loading. We expect that the frequency values from $f_{A\mu}^{(M)}/M$ should be less than those obtained by examining the differences between harmonics. In fact, we observe this consistently in our data analysis.

The next step is to examine the apparent mass loading. We could attempt to determine this jointly with the coupling through examination of the $f_{R\mu}^{(M)}$ data, but that is a rather complicated problem in multi-variable nonlinear optimization. Thus, here we choose to re-examine the series of $f_{A\mu}^{(M)}$, this time explicitly taking into account the non-zero mass loading. We have examined the $f_{A\mu}^{(M)}$ data from three different viewpoints: 1) using the $f_{A\mu}^{(M)}/M$ derived

$f_{A0}^{(1)}$, 2) using the harmonic difference derived $f_{A0}^{(1)}$, and then 3) determining a new $f_{A0}^{(1)}$ value that minimizes the standard deviation of the mass loading values. In fact, we were led to the latter approach by the inconsistencies in the indicated mass loading values using the first two approaches.

We subsequently added a fourth approach to determining $f_{A0}^{(1)}$, and then the mass loading. That is, we examined the $f_{R\mu}^{(M)}$ data to determine the value of $f_{A0}^{(1)}$ that minimized the standard deviation of the piezoelectric coupling values, under the assumption of zero mass loading, and then used this value with the $f_{A\mu}^{(M)}$ series to determine the effective mass loading. We were unsuccessful in any simplistic attempts to obtain optimal joint solutions for coupling, mass loading, and fundamental antiresonance frequency from the $f_{R\mu}^{(M)}$ data.

The indicated $f_{A0}^{(1)}$ obtained using these various approaches are listed in Tables V and VI. For any particular resonator, the extrema of the $f_{A0}^{(1)}$ values are separated by no more than 0.1%, therefore $f_{A0}^{(1)}$ is readily determined to three significant figures. In examining all of the possible interpretations of $f_{A0}^{(1)}$, we have obtained the most consistent results using the value of $f_{A0}^{(1)}$ that minimized the standard deviation of the piezoelectric coupling values obtained from the $f_{R\mu}^{(M)}$ data under the assumption of zero mass loading.

Using these values for $f_{A0}^{(1)}$, the effective mass loading values for the plates with Al electrodes are about 0.4%, while for those with Ag electrodes it is about 0.1%. It is unclear at this point what the proper interpretation is for these indicated mass-loading values.

As noted, the indicated values of $f_{A0}^{(1)}$ obtained from the $f_{R\mu}^{(M)}$ and $f_{A\mu}^{(M)}$ series were less consistent than hoped for. In all cases, the values of the indicated $f_{A0}^{(1)}$ were, in increasing order, first $f_{A\mu}^{(M)}/M$, then that from $f_{R\mu}^{(M)}$ while minimizing the standard deviation of the coupling, then that from the differences of $f_{A\mu}^{(M)}$ harmonics, and finally that from $f_{A\mu}^{(M)}$ while minimizing the variance of the mass loading. Again, it is unclear at this point what the proper interpretation is for this apparently systematic disagreement among the various interpretations.

TABLE V

INDICATED VALUES OF $f_{A0}^{(i)}$ USING DIFFERENT CRITERIA TO ANALYZE THE Al-ELECTRODED RESONATOR FREQUENCY SPECTRA.

Sample	$\left\langle \frac{f_{A\mu}^{(M)}}{M} \right\rangle$	$\left\langle \frac{f_{A\mu}^{(N)} - f_{A\mu}^{(M)}}{(N-M)} \right\rangle$	$f_{A0}^{(i)} _{\min(\sigma_\mu)}$	$f_{A0}^{(i)} _{\min(\sigma_k)}$
1	5077819	5082489	5082670	5079785
2	5071909	5076264	5076459	5073818
3	5065163	5071451	5071419	5066999
4	5061983	5066463	5066637	5063874

TABLE VI

INDICATED VALUES OF $f_{A0}^{(i)}$ USING DIFFERENT CRITERIA TO ANALYZE THE Ag-ELECTRODED RESONATOR FREQUENCY SPECTRA.

Sample	$\left\langle \frac{f_{A\mu}^{(M)}}{M} \right\rangle$	$\left\langle \frac{f_{A\mu}^{(N)} - f_{A\mu}^{(M)}}{(N-M)} \right\rangle$	$f_{A0}^{(i)} _{\min(\sigma_\mu)}$	$f_{A0}^{(i)} _{\min(\sigma_k)}$
1	4070556	4071849	4072157	4071369
2	4072787	4073973	4074270	4073574
3	4070207	4071271	4071586	4070979
4	4072836	4073999	4074294	4073633
5	4070631	4071793	4072107	4071107

TABLE VII

EFFECTIVE PIEZOELECTRIC COUPLING VALUES YIELDING MINIMUM σ_k FOR THE Al-ELECTRODED RESONATORS.

Sample	k (%) M=1	k (%) M=3	k (%) M=5	k (%) M=7	$\max(k)$ (%)	$\langle k \rangle$ (%)
1	14.28	15.44	13.56	14.99	15.44	14.57
2	14.28	15.21	13.90	14.78	15.21	14.54
3	14.40	15.29	14.13	14.85	15.29	14.67
4	14.40	15.30	13.91	14.91	15.30	14.63

TABLE VIII

EFFECTIVE PIEZOELECTRIC COUPLING VALUES YIELDING MINIMUM σ_k FOR THE Ag-ELECTRODED RESONATORS.

Sample	k (%) M=1	k (%) M=3	k (%) M=5	k (%) M=7	$\max(k)$ (%)	$\langle k \rangle$ (%)
1	13.45	13.92	11.13	14.54	14.54	13.26
2	13.38	13.94	11.18	14.47	14.47	13.24
3	13.34	13.57	10.47	14.77	14.77	13.04
4	13.41	13.49	10.44	14.83	14.83	13.04
5	13.36	13.06	7.86	11.40	13.36	11.42

The last step in examining the $f_{R\mu}^{(M)}$ and $f_{A\mu}^{(M)}$ series data was to determine the piezoelectric coupling values. We were unable to determine satisfactory values of $f_{A0}^{(i)}$ and μ that provided consistent values both for the $f_{A\mu}^{(M)}$ data and, with k, for the $f_{R\mu}^{(M)}$ data. We were only able to obtain somewhat consistent results by using the value of $f_{A0}^{(i)}$ that minimized the standard deviation of the piezoelectric coupling values obtained from the $f_{R\mu}^{(M)}$ data under the assumption of zero mass loading. The effective piezoelectric coupling values so obtained are listed in Table VII and VIII.

C. Extraction of Dielectric Constant and Modal Stiffness

The measured values of the static capacitance may be used to determine the dielectric permittivity ϵ_{11}^S . In so doing, however, we need to correct for a surprisingly large fringing field. The analysis of the two sets of samples is presented in Tables IX and X. The fringing field corrections are taken from [6]. For the samples with Al electrodes, we obtain $\epsilon_{11}^S = 18.15$, while for the samples with Ag electrodes we obtain $\epsilon_{11}^S = 18.10$. Both values are in excellent agreement with the “best fit” value of 18.19 reported recently in [7].

TABLE IX

DIELECTRIC CONSTANT ϵ_{11}^S VALUES FOR THE Al-ELECTRODED RESONATORS.

Sample	Uncorrected	2h/d _E	Correction Factor	Corrected
1	21.12	0.0394	1.135	18.60
2	20.27	0.0391	1.135	17.86
3	20.28	0.0392	1.135	17.87
4	20.75	0.0393	1.135	18.28

TABLE X

DIELECTRIC CONSTANT ϵ_{11}^S VALUES FOR THE Ag-ELECTRODED RESONATORS.

Sample	Uncorrected	2h/d _E	Correction Factor	Corrected
1	21.27	0.0486	1.163	18.29
2	20.98	0.0484	1.163	18.04
3	20.70	0.0483	1.163	17.80
4	21.31	0.0487	1.163	18.32
5	21.01	0.04869	1.163	18.07

The wave velocities for the various resonators are determined from the $f_{A0}^{(1)}$ and individual resonator thicknesses. The orientations differ slightly from each other, and a correction is applied to the data to bring all the values to a Y-cut reference. The samples with Al electrodes had an average wave velocity of 2787.85 m/sec, while the samples with Ag electrodes had an average wave velocity of 2765.79 m/sec. Both values are larger than the aggregate average value of 2757 m/sec from [7]. It is unclear at this point what the proper interpretation is for these differing indicated values, and whether the difference between them can provide an insight into the intrinsic stresses in the Al and Ag films.

The individual densities and wave velocities were then used to determine the effective elastic constant $c_{66}^D = c_{66}^E + e_{11}^2 / \epsilon_{22}^S$ for each resonator. The average value of c_{66}^D for the samples with Al electrodes was 43.47 GPa, while that for the samples with Ag electrodes was 43.95 GPa. Both values are in good agreement with the “best fit” value of 43.65 GPa [7].

D. Separation of Elastic and Piezoelectric Parts with Consideration of Energy Trapping

The least precise portion of the analysis is the final step wherein the effective coupling values are considered, and the effective stiffness is separated into elastic and piezoelectric parts. To do this, we take into account the underlying phenomenon wherein the observed coupling is an “effective” coupling value,

$$k_{eff}^2 = \Psi \cdot k^2 \quad (5)$$

where

$$\Psi \equiv \frac{\left[\frac{1}{A_e} \int_{A_e} g(r, \theta) r dr d\theta \right]^2}{\frac{1}{A} \int_A g^2(r, \theta) r dr d\theta} \quad (6)$$

is known as “Bechmann’s Psi.” This factor arises from the fact that, in a finite plate resonator, the electric field is uniform across the limited electrode region A_e , while the mechanical motion is non-uniform and may extend over the entire area of the plate A . As such, the conversion of electrical to mechanical energy is less than that associated with a uniform plane wave in an infinite piezoelectric medium by the indicated factor. The significance is this: we expect the coupling values to be less than or equal to the “true” coupling, and hence we select the maximum observed coupling as the best lower-bound estimate of the “true” coupling. We note that the measured “effective” coupling values (see Tables VII and VIII) for the samples with Al

electrodes are slightly higher than those for the samples with Ag electrodes, but both cases are somewhat lower than the theoretical value of $\sim 17\%$ from [7].

Under these assumptions, we analyze the data as shown in Tables XI and XII. We use the maximum observed “effective” coupling to separate the piezoelectrically stiffened elastic constant c_{66}^D into elastic and piezoelectric parts, recognizing that we are finding an upper limit for the elastic part and a lower limit for the piezoelectric part. The average values of $c_{66}^E = 42.44$ GPa for the samples with Al electrodes and 43.04 GPa for the samples with Ag electrodes are both in good agreement with the “best fit” value of 42.36 GPa [7]. The corresponding values for the piezoelectric constant e_{11} are 0.431 C/m² and 0.419 C/m². These values are somewhat less than the theoretical value from [7], but are fully consistent with the value of 0.426 C/m² obtained using resonant ultrasound spectroscopy [8].

We have used the theoretical value for $k \sim 17\%$ from [7] to calculate the implied values of “Bechmann’s Psi”. These values are also listed in Tables XI and XII. These values are consistent with the range of values expected for trapped energy resonators. There are two points of note in the data. First, the values of Ψ are larger for the samples with Al electrodes than for the samples with Ag electrodes, in spite of the nominally larger electrode mass loading for the samples with Ag electrodes. Second, we observe that the value of Ψ is noticeably lower for the sample that is a true Y-cut, and especially so for the higher harmonics.

TABLE XI
SEPARATION OF ELASTIC AND PIEZOELECTRIC PARTS FOR THE
Al-ELECTRODED RESONATORS

Sample	Orientation (minutes)	c_{66}^D (GPa)	c_{66}^E (GPa)	e_{11} (C/m ²)	Ψ
1	16.2	43.93	42.88	0.442	0.81
2	21	43.23	42.22	0.424	0.79
3	21.6	43.14	42.12	0.426	0.80
4	7.2	43.57	42.55	0.433	0.79

TABLE XII
SEPARATION OF ELASTIC AND PIEZOELECTRIC PARTS FOR THE
Ag-ELECTRODED RESONATORS

Sample	Orientation (minutes)	c_{66}^D (GPa)	c_{66}^E (GPa)	e_{11} (C/m ²)	Ψ
1	9.6	44.05	43.12	0.419	0.72
2	6.6	43.83	42.91	0.413	0.71
3	12.6	43.48	42.52	0.417	0.74
4	11.4	44.33	43.35	0.429	0.75
5	0'	44.08	43.29	0.383	0.60

IV. COMPARISON TO IEEE 176-1987

We have also analyzed the $f_{R\mu}^{(M)}$ and $f_{A\mu}^{(M)}$ data using the method recommended in IEEE 176-1987, i.e., taking the effective coupling of a particular harmonic as proportional to the difference between that specific resonance-antiresonance frequency pair. The results are shown in Tables XIII and XIV, where we have multiplied the observed IEEE 176-1987 coupling by the harmonic number in order to compare all harmonics on an equal basis. The coupling values derived using IEEE 176-1987 on a harmonic-by-harmonic basis are both less consistent and somewhat lower than those obtained using the finite plate analysis.

We have determined that the difference between the two approaches is caused by the differing approaches to determining the antiresonance frequencies. In IEEE 176-1987, the $f_{A\mu}^{(M)}$ are 1) presumed to be measured correctly on a harmonic by harmonic basis and 2) presumed to be adequately representative of $f_{A0}^{(1)}$. In the finite plate technique, the fit to multiple harmonics is used to derive a “best fit” estimate of $f_{A0}^{(1)}$, thereby both minimizing measurement errors and eliminating the implicit approximation. We have used the finite plate value of $f_{A0}^{(1)}$ along with the measured $f_{R\mu}^{(M)}$ data in a hybrid approach, and obtain results nearly identical to those obtained from the transcendental analysis. This further indicates that the discrepancy arises from the measurement of $f_{A\mu}^{(M)}$ and approximation of $f_{A0}^{(1)}$, as opposed to the linearization of the transcendental functions.

V. CONCLUSIONS

We have used the finite plate technique to analyze Y-cut langasite plan-parallel resonators with Al and Ag electrodes. We have extracted values for the piezoelectrically stiffened elastic stiffness c_{66}^D , the elastic stiffness c_{66}^E , the piezoelectric stress constant e_{11} , and the dielectric permittivity ϵ_{11}^S . The measured material constants are in very good agreement with other reported values.

We have also used the method recommended in IEEE 176-1987 to analyze these resonators. The method recommended in IEEE 176-1987 yields different values for the piezoelectric coupling than those obtained using the finite plate approach. We have determine that the difference between the two techniques lies in the assumptions and approximations used to determine the antiresonance frequencies.

TABLE XIII
EFFECTIVE PIEZOELECTRIC COUPLING VALUES
FOR THE Al-ELECTRODED RESONATORS USING IEEE 176-1987.

Sample	k (%) M=1	k (%) M=3	k (%) M=5	k (%) M=7	max(k) (%)
1	10.45	6.53	5.25	9.89	10.45
2	10.77	6.46	5.71	9.44	10.77
3	7.99	7.10	5.85	10.54	7.99
4	10.84	6.68	5.63	10.31	10.84

TABLE XIV
EFFECTIVE PIEZOELECTRIC COUPLING VALUES
FOR THE Ag-ELECTRODED RESONATORS USING IEEE 176-1987.

Sample	k (%) M=1	k (%) M=3	k (%) M=5	k (%) M=7	max(k) (%)
1	12.55	8.25	6.84	12.65	12.65
2	12.52	8.70	6.87	12.01	12.52
3	12.60	8.15	6.60	12.29	12.61
4	12.47	8.08	6.44	11.58	12.47
5	12.59	8.19	6.59	12.43	12.59

REFERENCES

- [1] ANSI/IEEE Standard 176-1987, “IEEE Standard on Piezoelectricity,” New York: IEEE, January 1988.
- [2] A. Ballato, “Transmission-line analogs for stacked piezoelectric crystal devices,” *Proceedings of the 26th Annual Frequency Control Symposium*, June 1974, pp. 229-236.
- [3] J. Kosinski, A. Ballato, and Y. Lu, “A finite plate technique for determination of piezoelectric material constants,” *IEEE Transactions on Ultrasonics, Ferroelectrics and Frequency Control*, vol. 43, no. 2, March 1996, pp.280-284.
- [4] S. Laffey, M. Hendrickson, and J. R. Vig, “Polished and etching langasite and quartz crystals,” *Proceedings of the 1994 IEEE International Frequency Control Symposium*, June 1994, pp. 245-250.
- [5] J. Kosinski, A. Ballato, I. Mateescu, and I. Mateescu, “Inclusion of nonuniform distribution of motion effects in the transmission-line analogs of the piezoelectric plate resonator: theory and experiment,” *Proceedings of the 1994 IEEE International Frequency Control Symposium*, June 1994, pp. 229-236.
- [6] Thomas H. Lee, “Derivation of Fringing Correction (Danger, Will Robinson – Integrals, Cheese and a Breeze Ahead!),” 1999.
- [7] J. A. Kosinski, R. A. Pastore, Jr., E. Bigler, M. P. da Cunha, D. C. Malocha, and J. Detaint, “A review of langasite material constants from BAW and SAW data: toward an improved data set,” *Proceedings of the 2001 IEEE/EIA International Frequency Control Symposium*, June 2001, pp. 278-286.
- [8] J. Schreuer, “Elastic and Piezoelectric Properties of La3Ga5SiO14 and La3Ga5.5Ta0.5O14: An Application of Resonant Ultrasound Spectroscopy,” *IEEE Transactions on Ultrasonics, Ferroelectrics and Frequency Control*, vol. 49, no. 11, November 2002, pp. 1474-1479.